

The Sun's small-scale magnetic elements in Solar Cycle 23

C. L. Jin, J. X. Wang, and Q. Song

*Key Laboratory of Solar Activity of Chinese Academy of Sciences
National Astronomical Observatories, Chinese Academy of Sciences, Beijing 100012,
China; cljin@nao.cas.cn; wangjx@nao.cas.cn*

and

H. Zhao

National Tsing Hua University, Hsinchu, Taiwan; berserker0715@hotmail.com

ABSTRACT

With the unique database from Michelson Doppler Imager aboard the Solar and Heliospheric Observatory in an interval embodying solar cycle 23, the cyclic behavior of solar small-scale magnetic elements is studied. More than 13 million small-scale magnetic elements are selected, and the following results are unclosed. (1) The quiet regions dominated the Sun's magnetic flux for about 8 years in the 12.25 year duration of Cycle 23. They contributed $(0.94 - 1.44) \times 10^{23}$ Mx flux to the Sun from the solar minimum to maximum. The monthly average magnetic flux of the quiet regions is 1.12 times that of active regions in the cycle. (2) The ratio of quiet region flux to that of the total Sun equally characterizes the course of a solar cycle. The 6-month running-average flux ratio of quiet region had been larger than 90.0% for 28 continuous months from July 2007 to October 2009, which characterizes very well the grand solar minima of Cycles 23-24. (3) From the small to large end of the flux spectrum, the variations of numbers and total flux of the network elements show no-correlation, anti-correlation, and correlation with sunspots, respectively. The anti-correlated elements, covering the flux of $(2.9 - 32.0) \times 10^{18}$ Mx, occupies 77.2% of total element number and 37.4% of quiet Sun flux. These results provide insight into reason for anti-correlated variations of small-scale magnetic activity during the solar cycle.

Subject headings: Sun: magnetic fields — Sun: photosphere — Sun: sunspots

1. Introduction

No any other astrophysical process but solar cycle leaves massive footprints on human’s living environment. This eleven-year cycle was discovered by a Germany pharmacist Schwabe (1843) from the number changes of solar sunspots. A primary understanding on the solar cycle has been established based on the theories and simulations of a mean-field magnetohydrodynamic (MHD) dynamo (Charbonneau 2005). However, new observations are continuously challenging our understanding by the myriad of new and seemingly conflicting observations. A more severe challenge comes from observations of small-scale magnetic elements (see de Wijn et al. 2009). Therefore, it is still a difficult task to explore the physics of solar cycle.

Since the 1960s it has been observed that small-scale magnetic fields outside of sunspots are everywhere on the Sun (Sheeley 1966, 1967; Harvey 1971). The stronger magnetic elements at the boundaries of supergranulation cells are network elements, while the smaller and weaker elements within the supergranulation cells are intra-network (IN) elements (Livingston & Harvey 1975; Smithson 1975). Similar to emerging flux regions (EFRs) in sunspot groups (or active regions) (Zirin 1972), small-scale emerging bipoles named ephemeral (active) regions (ERs) were described by Harvey and Martin (1973). They account for the formation of network elements in addition to the debris from decaying sunspots. It was noticed that the flux emerging rate in ER exceeds that in sunspots by two orders of magnitude (Zirin 1987). Moreover, flux generation rate of IN elements exceeds that of ERs by another two orders of magnitude. Further smaller magnetic fibrils are believed to be mostly unresolved by present telescopes, yet their aggregation is the dominant mechanism by which IN and network elements appear (Lamb et al. 2008). A substantial amount of solar magnetic flux is probably still hidden (Trujillo et al. 2004).

As soon as the small-scale magnetic elements were identified, great efforts have been made to understand how they change during a solar cycle and if they are correlated with sunspots. Diverse observations are reported, igniting discussions and debates in the literature. The observations are made either directly from the magnetic measurements, or indirectly from proxies of small-scale magnetic flux, e.g., the G-band and CaII K bright points and coronal X-ray bright points. Key revelations are listed below.

- (1) No cyclic variations: CaII K emission in solar quiet regions (White & Livingston 1981); modern X-ray bright points observations (Sattarov et al. 2002; Hara & Nakakubo 2003); magnetic flux of networks (Labonte & Howard 1982); flux spectrum and total flux of network elements with flux $\leq 2.0 \times 10^{19}$ Mx (Hagenaar et al. 2003); Stokes $\frac{Q}{I}$ profile (Trujillo et al. 2004).

- (2) Anti-correlation of small-scale fields with sunspot cycle: number of network bright points in very quiet regions (Muller & Roudier 1984, 1994); HeI 10830 Å dark points in the higher chromosphere (Harvey 1985); early X-ray bright points observations (Davis et al. 1977; Davis 1983; Golub et al. 1979); Weak changes of emergence frequency of ERs with flux less than $(3-5) \times 10^{19}$ Mx (Hagenaar et al. 2003).
- (3) Correlation with sunspot cycle: more ERs appeared during active solar condition (Harvey & Harvey 1974; Harvey 1989); the number (or magnetic flux) of network structures (Foukal et al. 1991; Meunier 2003); flux distribution and total flux of network concentrations with flux $(2.0 - 3.3) \times 10^{19}$ Mx (Hagenaar et al. 2003).

The observations listed above are related to some fundamental, but not yet resolved questions in solar physics: the origin, dynamics and active role in Sun’s global processes of solar small-scale magnetic elements, as well as the controlling physics of solar activity cycle. However, discrepancy among different authors is not yet understood, implying problems either in the observations or on the physics used to interpret the observations. A few aspects make things even more complicated.

First, for the observations of the proxies of small-scale magnetic elements, the connections between the magnetic elements and their proxies are not well quantified, and the underlined physics is not known exactly. There seems to be not a one-to-one correspondence between network elements and network bright points (Zhao et al. 2009). In other words, the widely-adopted paradigm of “magnetic bright points” is still questionable. Moreover, the early revelation about the magnetic properties of coronal X-ray bright points (Golub et al. 1977), needs to be revisited and updated with state-of-the-art observations.

Secondly, quite many reports listed above went back to early solar observations, which makes us difficult to evaluate the quality of the observations. We are confused by rather poor resolution, calibration and consistency in sensitivity in early magnetic measurements. As an example, the early Mont. Wilson magnetograph observations (Labonte & Howard 1982) were with a resolution of $\geq 12.5-17.5$ arcsec, and the calibration was not consistent time to time. We are simply not able to say anything confidently about their conclusions. Additionally, early X-ray bright point measurements, which suffered from low cadence, purported to show a decrease in the number of X-ray bright points with the solar cycle. More recent higher cadence observations have called into question whether this effect is real. It reminds to be seen whether other observations of variation with the solar cycle also need to be reinterpreted. New observations with careful and thorough data reduction and interpretation are crucially required.

Thirdly, even for recent observations, sometimes, the different algorithm and logic in

data analysis make us hard to judge the results too. An interesting example comes from the analysis of full-disk magnetograms of the Michelson Doppler Imager aboard the Solar and Heliospheric Observatory (MDI/SOHO) (Scherrer et al. 1995). By adopting the different detection algorithm and approaches, Meunier (2003) revealed correlation of the network element number (or flux) with sunspots; in contrast, Hagenaar et al. (2003) declared some weak anti-correlated emergence rate of ERs and an independence of the total absolute flux for smaller network concentrations. This discrepancy should be clarified with new analysis.

To clarify the problem and to close the debates are an essential task in understanding the solar cycle phenomena. Fortunately, now MDI/SOHO is providing a unique database - the full-disk magnetograms over more than 13 years, covering the complete 23rd Solar Cycle. The 13.5 year 5-min average full disk magnetograms are used in the current study. However, the poor temporal resolution makes the identity of ERs questionable and the sensitivity of the full-disk magnetograms rules out the possibility to resolve the IN elements. Therefore, what we have identified in this study is basically the network magnetic elements.

In this paper, we aim at learning the cyclic variations of quiet Sun’s magnetic flux and small-scale magnetic elements. To use the full-disc MDI magnetograms with the temporal coverage of entire Cycle 23 comes from an awareness of the intermittency of solar cyclic behavior in both the temporal and spatial domains. By the intermittency to select the magnetograms of a short interval, e.g., 10-30 hours, in a month for each year, at the ‘supposed’ different cycle phases. would not guarantee a grape of the key characteristics of a solar cycle. From our understanding, to choose the database that cover the entire cycle 23 is of overwhelming importance. The database for the current study is unique in the sense that it is the only space-borne magnetic measurements of the full Sun, for which the consistency in sensitivity and resolution persisted for a cycle-long interval. As we are interested in the global behavior of small-scale magnetic elements, sampling network elements in a cycle-long temporal domain and in all different flux ranges (or strengths) are more important than selecting a few high cadence sequences interruptedly. Moreover, the magnetic elements with different flux (or size) may have different origins and characteristics, therefore we group all the network magnetic elements into different categories in accordance with their magnetic flux.

In section 2, we describe the observations, the technique of calibration, the evaluation of noise level of the magnetograms, the separation of active regions and the quiet Sun, and the selection of network elements. In section 3, we present the results of cyclic behavior of quiet region magnetic flux and small-scale magnetic elements. In section 4, we make the comparison with previous studies, and consider the possibilities on how to understand the anti-correlated network magnetic elements with sunspots. In section 5, we draw the

conclusions.

2. Observations and methods

The MDI instrument aboard SOHO spacecraft provides the full-disk magnetogram with a pixel size of $2''$. In order to obtain a low noise level, only those 5-min average magnetograms are selected in the study. We extract one observed full-disk magnetogram per day, and thusly we totally select 3764 magnetograms from 1996 September to 2010 February, which include the complete 23rd solar cycle. In order to further reduce the noise level, we apply a boxcar smoothing function to each magnetogram by a width of $6'' \times 6''$. There are two groups of authors who first pointed out the under-estimation of magnetic flux by earlier MDI full-disk magnetogram calibration (Berger et al. 2003; Wang et al. 2003). All the magnetograms used in this study are that retrieved after recalibration of December 2008. For a better understanding about the cyclic behavior of solar minima of Cycles 22 and 23, we extend the MDI data base by adding Kitt Peak full-disk magnetograms from August 1996 back to January 1994. The data merging is made based on a least-square fitting of the mean flux density of Kitt Peak magnetograms to that of MDI magnetograms for the common interval of 1996.

We estimate the noise level of these smoothed 5-min average magnetograms according to the method described by Hagenaar (2001) and Hagenaar et al. (2003). Based on these magnetograms, we analyze their histograms of magnetic flux density. The core of the distribution function is fitted by a Gaussian function $F(x) = F_{max} \exp(-x^2/2\sigma^2)$, where the width σ of the Gaussian function, about 6 Mx/cm^2 , is defined as the noise level.

We assume that the observed line of sight magnetic flux density is a projection of the intrinsic flux density normal to the solar surface, so the magnetic flux density for each pixel is corrected (see Hagenaar 2001 and Hagenaar et al. 2003) as $B_{cal} = B_{obs}(\alpha)/\cos(\alpha)$. The angle α of each pixel is defined by $\sin(\alpha) = \sqrt{x^2 + y^2}/R$ Where x and Y are the pixel position referring to the disk center, at which x and y is equal to 0, and the R is the solar disk radius. After the correlation, the magnetogram shows the magnetic flux density normal to solar surface.

After the angle is greater 60 degrees, there are less and less magnetic signals due to the lower magnetic sensitivity and spatial resolution of MDI/SOHO magnetograms, and the magnetic noise level would increase according to the magnetic correction $1/\cos(\alpha)$. Therefore, we only analyze these pixels with angle α less than 60 degree, i.e., the region included by the black circle in the left panels of Fig. 1. The flux density of the pixel with $60^\circ \leq \alpha \leq 90^\circ$

is set to zero.

For each smoothed and corrected full-disk magnetogram of MDI/SOHO, we apply a magnetic flux density of 15 Mx/cm^2 as a threshold to define the active regions and their surroundings, and then create a mask for each magnetogram. These masks include many small clusters and isolated pixels, so only the islands with area larger 9×9 pixels are defined as the active regions (Hagenaar et al. 2003). Considering the active regions close to the edge of 60 degree, in order to avoid missing them in the automatic procedure, we always search the active regions in the solar disk with angle α less than 70 degree first, as that shown in the left panels of Fig. 1. Thusly, the islands with area less than 81 pixels within 60 degree disk are still defined as the active regions if they have more than 81 pixels searched within 70 degree disk.

Two magnetograms within the 70deg from disk center at approximately the solar maximum and minimum phases, respectively, are displayed in the left panels of Fig. 1. On these retrieved magnetograms the selected ARs are masked by red curves. The criterion of selecting ARs appears to work well from a visually examination for the given cases. In the right panels two selected sub-windows of the magnetograms are shown with contours outlining the network elements which are selected by a procedure of automatic feature selection. The yellow and green contours outline the selected network elements that are belong to the components of correlated and anti-correlated with sunspots in the solar cycle, respectively (see Section 3.2).

3. Results

3.1. Cyclic variations of magnetic flux of solar quiet regions

In order to compare the cyclic variations of magnetic flux of active regions with that of quiet regions, we calculate their magnetic flux, respectively, which is shown in the left panel of Fig. 2. At the same time, the area ratio of quiet regions is also computed, which is shown by purple '+' symbols in the right panel of Fig. 2. It is found that the quiet Sun contributed $(0.94 - 1.44) \times 10^{23} \text{ Mx}$ flux from approximately the solar minimum to maximum in Cycle 23. The fractional area of quiet regions always exceeds 80% in the entire solar cycle 23, and decreased from the cycle minimum to maximum by a factor of 1.2, although their total flux increased by a factor of 1.53; as a comparison, the active region flux increased by several orders of magnitude. The measurements confirm the global behavior of the quiet Sun fields (see Meunier 2003 and Hagenaar et al. 2003). During the 12.25 years of Cycle 23, from October 1996 to December 2008 (see <http://www.ips.gov.au>), the quiet Sun dominated

the Sun's magnetic flux for 7.92 years. The monthly average magnetic flux of quiet Sun is 1.12 times that of active regions. The magnetic fields on the quiet Sun, indeed, are a fundamental component of the Sun's activity cycle which maintains the Sun's magnetic energy and Poynting flux at a certain level.

It is interesting to notice that the ratio of the quiet Sun's magnetic flux to solar total flux (referring to as the flux occupation by the quiet Sun) equally characterizes the course of a solar cycle, like sunspots. The occupation of 6-month running-average magnetic flux by the quiet Sun is shown by purple cross symbols in the right panel of Fig. 2. The active region flux shown in the left panel answers for the variation of sunspot cycle very well. However, for the quiet regions, the maximum occupation of magnetic flux marks the minima of solar cycles. For instance, in our data set, the maximum flux occupation of quiet Sun, which was 96.0%, first happened in October of 1996 at the beginning of Cycle 23. The later maxima happened from July 2008 to August 2009. In December of 2008, the beginning of Cycle 24, the maximum occupation reached 99.3%. The 6-month running-average fractional flux of quiet Sun had been larger than 90.0% for 28 continuous months (from July 2007 to October 2009), which characterizes the grand solar minima of Cycles 23-24. Staying at such a low activity level there were 25 months, for which the total AR flux was less than 10^{22} Mx. However, during the minima of Cycles 22-23 for only intermittent 7 months, i.e., from December 1995 to April 1996 and from December 1996 to January 1997, we had witnessed the fraction larger than 90.0%. The distinction between two solar minima are so severe, which can be seen very clearly in Fig. 2.

3.2. Cyclic variations of network magnetic elements

After excluding the active regions, we apply the magnetic noise, i.e., 6 Mx/cm^2 as a threshold to create a mask for each quiet magnetogram, and define these magnetic concentrations with more than 10 pixels in size as network magnetic elements (Hagenaar et al. 2003). More than 13 million network elements have been identified for the interval from September 1996 to February 2010. The probability distribution function (PDF) of these magnetic elements in the studied interval is shown in Fig. 3 as the average flux distribution. From the figure, it can be found that the distribution of magnetic flux of network magnetic elements mainly concentrate at the flux of 10^{19} Mx. This peak distribution is consistent with that found for multiple MDI full-disk datasets by parnel et al. (2009) (see their Fig. 5)

For an exclusive examination, we divide all the magnetic elements into 96 sub-groups according to the flux per element. In this way, a statistical sample is created, covering the range of magnetic flux per element from the smallest observable network flux of 1.5×10^{18}

Mx for the current data set to an upper limit of 3.8×10^{20} Mx. The monthly variation of magnetic elements for each sub-group is calculated and examined in term of number density and absolute total flux in the interval from October 1996 to February 2010, embodying the entire Cycle 23. The influence of the area changes of the quiet Sun on both quantities has been removed. There are 0.3% of network elements (or clusters) with flux larger than the upper limit, which were fragments of decayed sunspots and not included in the sample. By following Hagenaar et al. (2003) tiny flux pieces with less than 10 pixels are not considered in the study. As a whole the total flux of these tiny flux pieces showed a small variation in the scope of $(3.5 - 4.0) \times 10^{22}$ Mx during the cycle.

The correlation coefficients between the cyclic variation of numbers of network elements and sunspots are calculated for each sub-group of network elements and shown in Fig. 4. They are the linear Pearson correlation coefficients of two vectors for each sub-group elements. Denote the element number in sub-group i as N_i and the sunspot number N_s , then the correlation coefficient between N_i and N_s will be

$$\rho(N_i, N_s) = \text{Covariance}(N_i, N_s) / (\text{Variance}N_i \times \text{Variance}N_s)^{\frac{1}{2}} \quad (1)$$

The confidence level about the correlation can be found in some basic statistics handbook by taking account of how big was of the sample. As the sample size for each sub-group elements is 162, which is quite large. If the coefficient is higher than 0.256, then the failure probability of the linear correlation would already be < 0.001 .

From the small to the large flux spectrum, there appears a remarkable 3-fold correlation scheme between the network elements and the sunspots: basically no-correlation, anti-correlation and correlation. This behavior is held for both the element number and total flux. Either the anti-correlation or the correlation has been observed at very high confidence level. The majority of the correlations show a failure probability ≤ 0.001 . Between the anti-correlation and correlation, there is a narrow range of magnetic flux per element of $(3.2 - 4.3) \times 10^{19}$ Mx. Network elements falling in this flux range show a transition from anti-correlation to correlation with sunspot cycle (see the narrow shaded column in the middle of Fig. 4.)

The dependence of the correlation coefficient on the element flux hints the possibility that network elements at different segments of the flux spectrum may present different physical origins and different cyclic behavior accordingly. For an detailed examination of cyclic behavior of network elements, we group all the network elements into 4 categories which show, respectively, no-correlation, anti-correlation, transition from anti-correlation to correlation, and correlation with sunspot cycle. For each category, its flux range, percentage in

number and in total flux, as well as the correlation coefficient with sunspots are listed in Table 1. We, then, discriminate the cyclic variation of magnetic elements in accordance to the flux range listed in the table. The detailed cyclic variations of each category network elements are shown in Fig. 5.

Approximate 77.2% of the magnetic elements, covering the flux range of $(2.9-32.0)\times 10^{18}$ Mx show anti-correlation with the sunspot cycle. This anti-correlated component contributes 37.4% of network flux during Cycle 23. Transition from anti-correlation to correlation takes place between $(3.20 - 4.27) \times 10^{19}$ Mx. The correlated component elements have magnetic flux larger than 4.27×10^{19} Mx. They occupy approximately 15.7% in number but 53.5% of total flux of network elements. In the flux range of $(1.5-2.9)\times 10^{18}$ Mx, network elements show randomly independent variation with the sunspot cycle. From this data set, they occupy less than 0.6% of network elements and have neglectable total flux. With the poor sensitivity in flux measurements at the smallest end of the flux spectrum, it could not be excluded that the non-correlation component manifested some random noises in flux measurement. More serious efforts with higher resolution and sensitivity data are necessary to clarify the cyclic behavior of smallest observable magnetic elements.

The number changes of the network elements in the flux range of $(2.9 - 32.0)\times 10^{18}$ Mx show obviously anti-phase correlation with sunspot cycle, so do the changes of their total unsigned flux. However, the cyclic minimum of this anti-correlation component is not exactly coincided with the reversed profile of the maximum of the sunspot cycle, implying complexity in causing the anti-correlation. Meanwhile, the flux changes of the magnetic elements with flux larger than 4.3×10^{19} Mx show remarkable in-phase correlation with sunspot cycle. The same is true that the profiles of the maximum of network elements and that of sunspots are not corresponding one another exactly. There is a 5-7 month delay of their cyclic maximum related to that of the sunspot cycle. This seems to be related to the characteristics dispersal time of active region fields.

To further explore the cyclic variation of magnetic elements, we obtain the PDFs of yearly network magnetic elements according to the magnetic flux, and compute the differential PDFs, i.e., the difference between the yearly PDFs and average PDF (see Fig.3). Here, the differential probability distribution function is abbreviated as DPDF. We plot the DPDFs, and show the variation for magnetic flux spectrum from 1996 to 2010 in Fig. 6. From the figure, we confirm the 3-fold scenario of cyclic variations of network elements.

From the solar minimum to solar maximum (see the first column of the figure), the distribution of magnetic elements in the flux range about $(3-30)\times 10^{18}$ Mx gradually decrease, which shows the anti-correlation variation with the sunspot cycle; while the distribution of magnetic elements of flux larger than about 4×10^{19} shows the correlation variation with

the sunspot cycle and reaches the peak in the years 2000, 2001 and 2002. Furthermore, the distribution of magnetic elements with flux of $\sim 3 \times 10^{19}$ and less than 3×10^{18} Mx shows almost no variation. The distribution of magnetic elements correlated with the sunspot cycle reaches the smallest values in the years 2007, 2008 and 2009, which are the solar minima of cycle 23-24; while the distribution of magnetic elements anti-correlated with the sunspot cycle shows outstanding peak during this long interval (see the third column of the figure). The distribution characterizes the long duration of the solar minima of Cycles 23-24. It is noticed that the distributions in some of the ascending and declining phases (see that in 1998 and 2005) are, more or less, represent the average distribution of small-scale magnetic elements shown in Fig.3.

4. Discussion

With the unique space-borne observations which comprised a complete solar cycle, we have revealed a 3-fold correlation scheme of the Sun's small-scale magnetic elements with sunspot cycle, and identified an anti-correlation component of network elements that dominates the element population. Before coming up with conclusion and discussion on the physics, a comparison with previous studies that adopted the similar approaches and with that same space-borne MDI observations (see Section 2) is necessary.

Hagenaar et al.(2003) selected high cadence magnetograms of 6 time-sequences, each of which covered 10-30 hours in a month from 1996 to 2000. These authors found that the component of network elements with flux $\geq 30 \times 10^{18}$ Mx varied in phase with the sunspot cycle. The magnetogram calibration they adopted had under-estimated the flux density by a factor of about 1.6 (Bergers et al. 2003; Wang et al. 2003). With the renewed calibration, this component would consist of magnetic elements with flux $\geq 4.8 \times 10^{19}$. This is a component in our analysis that changes in phase with sunspots. Meunier (2003) chose strong magnetic elements with threshold flux density of 25 G and 40 G, respectively, and found naturally a correlation of number and flux of network elements with sunspots.

When the element flux $\leq 20 \times 10^{18}$ Mx (i.e., 32×10^{18} Mx in renewed calibration), Hagenaar et al.(2003) declared that both the flux spectrum of quiet network elements and the total flux changed a little with the cycle phase. These authors used the interrupted data in the 6 years of the ascending cycle phase, they would not be able to guarantee a grasp of the real trend of the cyclic modulation. We tested their results by using the same 6-month 5-m magnetograms, and found a weak change, but anti-phased with the cycle phase, in both numbers and flux for network elements in this flux range. In fact, Hagenaar et al.(2003) reported that the number density of network concentrations on the quiet Sun decreased by

less than 20% from 1997 to 2000, consistent with our approaches. They also suggested an even anti-correlated changes in flux emergence rate in this low flux range. The revelation of a remarkable anti-correlation component of network elements with a broad flux range from several times of 10^{18} Mx to 3 times of 10^{19} Mx is likely to be the true nature of small-scale solar magnetism and inspiring new considerations of the Sun’s magnetism.

Exploration of the magnetic nature of the Sun’s small-scale activity went back to earlier solar studies. A few pioneer studies stand still as reliable references in solar physics. Mehlretter (1974) identified that the network bright points represented magnetic flux concentration with field strength of 1000-2000 G, each of them had a mean flux of 4.7×10^{17} Mx. Later, the work was extended by Muller & Roudier (1984, 1994). They deduced an average flux of 2.5×10^{17} Mx for an network bright points. The flux range suggested by these authors for the network bright points changing anti-phased with sunspot cycle, is out of reach by current data base. Muller & Roudier (1984) also identified the correlation between the network bright points in the photosphere and coronal XBPs. For the latter, Golub et al.(1977) carefully studied their magnetic properties, and found the average total flux associated with a typical XBP was 2.0×10^{19} Mx. The magnetic measurements were obtained at Kitt Peak with a fine scan of 2.5 arcsec resolution element and ~ 2 G noise level. They are reasonably reliable to quantify the magnetic flux of an XBP. This typical flux, even with some uncertainty, e.g., 50% or larger, is still falling in the flux range of the anti-correlated component of network elements discovered by this study. We tentatively suggest that the anti-correlated component of magnetic elements are responsible for the small-scale activity, e.g., the coronal X-ray bright points. Updated efforts to quantify the magnetic properties of the so-called magnetic bright points are crucial to final resolve the long-lasting puzzle of the anti-phase behavior of the Sun’s small-scale activity in a solar cycle.

Observationally, small-scale network elements come from several sources: fragmentation of active regions, flux emergence in the form of ephemeral regions, coalescence of intranetwork flux, and products of dynamic interaction among different sources of magnetic flux. The 3-fold relationship between network elements and sunspot cycle has immediate implication on the Sun’s magnetism. As demonstrated by state-of-the-art simulations (see Vögler & Schüssler 2007), the magnetic elements at the smallest end of the flux spectrum, either resolved or un-resolved, manifest a local turbulent dynamo which operates in the near-photosphere and is independent to the sunspot cycle. On the other hand, at the larger flux end, the magnetic elements are likely to be the debris of decayed sunspots. They follow, of course, the solar cycle.

The key issue here is how to understand the majority of magnetic elements which are anti-correlated with sunspots in the solar cycle. They are not likely the debris of decayed

sunspots, but probably created by turbulent local dynamo action that, however, is globally affected or controlled by the sunspot field from the mean-field MHD dynamo. A few possibilities now are being considered.

First, during the more active times of the Sun, the smaller magnetic elements created by the turbulent dynamo have more opportunity to encounter sunspots and their fragments. The same-polarity encountering results in a merging of those elements to the flux related to sunspots. Whereas, the opposite polarity encountering causes flux cancelations with the net results of lost smaller elements and a diffusion of sunspot flux. What accompanied the sunspot flux diffusion is the reduced smaller elements with the turbulent origin. This accounts for the anti-correlated magnetic component possibly. By this kind of interaction magnetic flux from turbulent dynamo actively takes part in the operation of the solar cycle, helping with more efficient magnetic diffusion. To quantify this mechanism, studies of dynamic interaction between small-scale magnetic elements and active regions fields are crucially required.

Secondly, it is also possible that at the solar maximum, the stronger magnetic field from sunspots tends to suppress the Sun's global convection in some measure. As a result, the local dynamo has been abated somehow, and the network elements created by turbulence are reduced in number and total flux. This seems to suggest that the turbulent dynamo is, in fact, global but not local. Unfortunately, so far there have been no definite observations about the changes in the global solar convection during the sunspot cycle.

Another possibility is that the anti-correlated component represents the recycling of parts of the previously diffused or submerged magnetic flux from the mean-field dynamo (Parker 1987). The diffusion of magnetic flux from sunspots to the deep convection zone requires 5-7 years (Jiang et al. 2007). Parts of the diffused or submerged flux serves as the seed field for the globally turbulent dynamo. Its production is naturally out of phase with sunspots in the solar cycle, and brings up the magnetic elements that anti-phased with sunspots.

In a recent literature, Thomas and Weiss (2008) proposed a picture of the solar Dynamo on three scales (one large and two small), which, according to the above authors, were only loosely coupled to each other. It is not clear if some unknown interplay of different scale dynamos may result in the complicated behavior of the Sun's small-scale fields. If we adopt the common vision that the smaller magnetic elements are created by a local turbulent dynamo, then the local turbulent dynamo on a certain scale must have closely correlated to the global mean-field dynamo. The global dynamo either provides seed flux or modifies the condition for this 'global' turbulent dynamo. At the smallest end, the dynamo is likely to be more 'local'. The turbulent dynamo, either global or purely local, brings a tremendous

amount of turbulent flux to the Sun that continuously interacts with the products of the mean-field dynamo. The interaction seems to not only help with the operation of the global dynamo, but also power the ceaseless small-scale magnetic activity and maintain the Sun’s Poynting flux to Earth and interplanetary space.

5. Conclusions

With the unique database from MDI/SOHO in the interval from September 1996 to February 2010, which embodies the entire Solar Cycle 23, we analyze the cyclic variations of quiet Sun’s magnetic flux and Sun’s small-scale magnetic elements.

The quiet regions contributed $(0.94 - 1.44) \times 10^{23}$ Mx flux from approximately the solar minimum to maximum in Cycle 23. The fractional area of quiet regions decreased from the cycle minimum to maximum by a factor of 1.2, but their total flux increased by a factor of 1.53. The quiet regions dominate Sun’s magnetic flux over 60% duration of the cycle. Furthermore, the ratio of the quiet region magnetic flux to the Sun’s total flux can be used to describe the course of solar cycle, just as sunspots. The maximum flux occupation of quiet regions marks the minima of solar cycle. The flux occupation on the quiet Sun had been larger than 90% for 28 continuous months from July 2007 to October 2009, which seems to equally characterize the grand minima of Cycles 23 and 24.

With increasing magnetic flux per element the number and total flux of the Sun’s small-scale magnetic elements follow no-correlation, anti-correlation and correlation changes with sunspots. The anti-correlated component, covering the flux range of $(2.9 - 32.0) \times 10^{18}$ Mx, occupies 77.2% of total elements and 37.4% of flux on the quiet Sun. However, the stronger magnetic elements with flux larger than 4.3×10^{19} Mx dominate the quiet Sun magnetic flux and follow closely the sunspot cycle.

The definitively identified anti-correlated component of the small-scale magnetic elements seems to offer an interpretation on the puzzling observations of anti-correlation variation of many types of small-scale activity with the solar cycle, e.g., the network bright points, HeI 10830 Å dark points and coronal X-ray bright points.

It is speculated that the anti-correlated small-scale magnetic elements are products of some local turbulent dynamo or dynamos that is modulated to be anti-phased with the global mean-field dynamo.

The authors are grateful to Dean-Yi Chou, Sara Martin and Jie Jiang for their valuable suggestions and discussions. We appreciate the instructive advice and valuable suggestions

of the anonymous referee, by which the paper has been significantly improved. The work is supported by the National Natural Science Foundation of China (10873020, 11003024, 40974112, 40731056, 10973019, 40890161, 10921303, 11025315), and the National Basic Research Program of China (G2011CB811403).

REFERENCES

- Berger, T. E. & Lites, B. W. 2003, *Sol. Phys.*, 213, 213
- Charbonneau, P. 2005, *Living Reviews in Solar Physics*, 2, no.2
- Davis, J. M. 1983, *Sol. Phys.*, 88, 337
- Davis, J. M., Golub, L., & Krieger, A. S. 1977, *ApJ*, 214, L141.
- de Wijn, A. G., Stenflo, J. O., Solanki, S. K., & Tsuneta, S. 2009, *Space Sci. Rev.*, 144, 275
- Foukal, P., Harvey, K., & Hill, F. 1991, *ApJ*, 383, L89
- Golub, L., Krieger, A. S., Harvey, J. W., Vaiana, G. S. 1977, *Sol. Phys.*, 53, 111
- Golub, L., Davis, J. M. & Krieger, A. S. 1979, *ApJ*, 229, L145
- Hagenaar, H. J. 2001, *ApJ*, 555, 448
- Hagenaar, H. J., Schrijver, C. J., & Title, A. M. 2003, *ApJ*, 584, 1107
- Hara, H., & Nakakubo, K. 2003, *ApJ*, 589, 1062
- Harvey, K. 1985, *Aust. J. Phys.*, 38, 875
- Harvey, K. 1989, *Bull. American Astron. Soc.*, 21, 839
- Harvey, K., & Harvey, J. 1974, *Bull. American Astron. Soc.*, 6, 288
- Harvey, K., & Martin, S. F. 1973, *Sol. Phys.*, 32, 389
- Harvey, J. 1971, *Publ. Astron. Soc. Pacific*, 83, 539
- Jiang, J., Chatterjee, P., & Choudhuri, A. R. 2007, *MNRAS*, 381, 1527
- Labonte, B. J., & Howard, R. 1982, *Sol. Phys.*, 80, 15
- Lamb, D. A., et al. 2008, *ApJ*, 674, 520

- Livingston, W. C., & Harvey, J. 1975, *Bull. American Astron. Soc.*, 7, 346
- Mehltretter, J. P. 1974, *Sol. Phys.*, 38, 43
- Meunier, N. 2003, *A&A*, 405, 1107
- Muller, R., & Roudier, T. 1984, *Sol. Phys.*, 94, 33
- Muller, R., & Roudier, T. 1994, *Sol. Phys.*, 152, 131
- Nakakubo, K., & Hara, H. 2000, *Adv. Space Res.*, 25, 1905
- Parker, E. N. 1987, *Sol. Phys.*, 110, 11
- Parnell, C. E., DeForest, C. E., Hagenaar, H. J., Johnston, B. A., Welsch, B. T. 2009, *ApJ*, 698, 75
- Sattarov, I., Pevtsov, A. A., Hojaev, A. S., & Sherdonov, C. T. 2002, *ApJ*, 564, 1042
- Scherrer, P. R. et al. 1995, *Sol. Phys.*, 162, 129
- Schwabe, M. 1843, *AN*, 20, 283
- Sheeley, N. R. Jr. 1966, *ApJ*, 144, 723
- Sheeley, N. R. Jr. 1967, *Sol. Phys.*, 1, 171
- Smithson, R. C. 1975, *Bull. American Astron. Soc.*, 7, 346
- Thomas, J. H., & Weiss, N. O. 2008, *Sunspots and Starspots*, Cambridge Univ. Press
- Trujillo Bueno J., Shchukina, J. N., & Asensio Ramos, A. 2004, *Nature*, 430, 326
- Vögler, A., & Schüssler, M. 2007, *A&A*, 465, L43
- Wang, J., Zhou, G., Wang, Y., Song, L. 2003, *Sol. Phys.*, 216, 143
- Webb, D. F., Martin, S. F., Moses, D., Harvey, J. W. 1993, *Sol. Phys.*, 144, 15
- White, O. R., & Livingston, W. C. 1981, *ApJ*, 249, 798
- Zhao, M., Wang, J. X., Jin, C. L., & Zhou, G. P. 2009, *RAA*, 9, 933
- Zirin, H. 1972, *Sol. Phys.*, 22, 34
- Zirin, H. 1987, *Sol. Phys.*, 110, 101

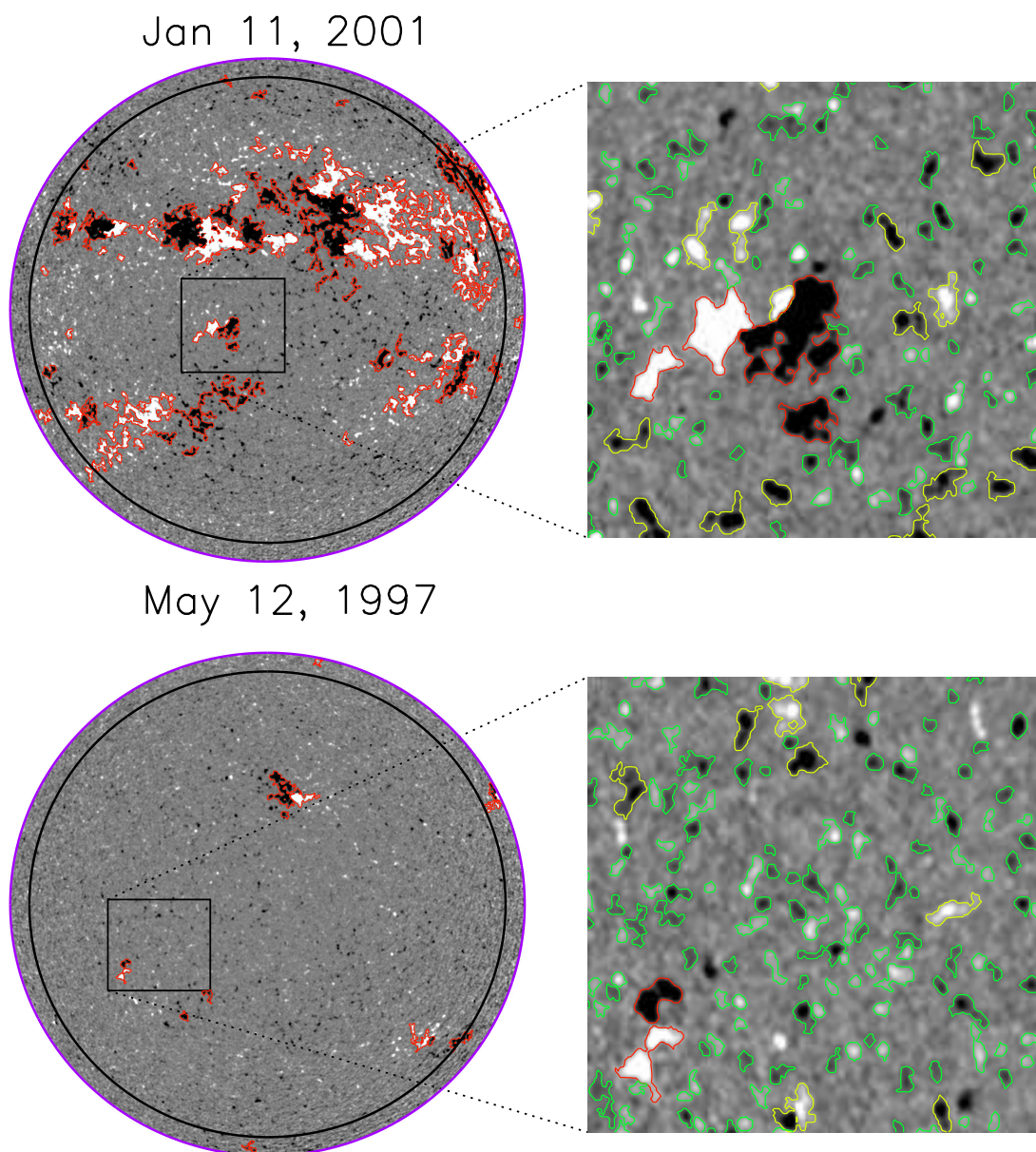


Fig. 1.— Left panels: Two retrieved MDI 5-minute full-disk magnetograms within 70 deg from disk center, at approximately the solar maximum and minimum, respectively. Using the threshold on 15 Mxcm^{-2} to define the edge of active region, the islands with area larger 9×9 pixels, i.e., the regions contoured by red line, is defined as active regions. The purple circle displays the location $\alpha=70$ deg, and the black circle displays the location $\alpha=60$ deg. The gray scale saturates at $\pm 50 \text{ Mxcm}^{-2}$. Right panels: enlarged images for the windows framed in the MDI magnetograms, on which network elements falling in the flux ranges of $(2.9\text{-}32.0) \times 10^{18} \text{ Mx}$ and $(4.3\text{-}38.0) \times 10^{19} \text{ Mx}$ are outlines by green and yellow curves, respectively (see Section 3.2).

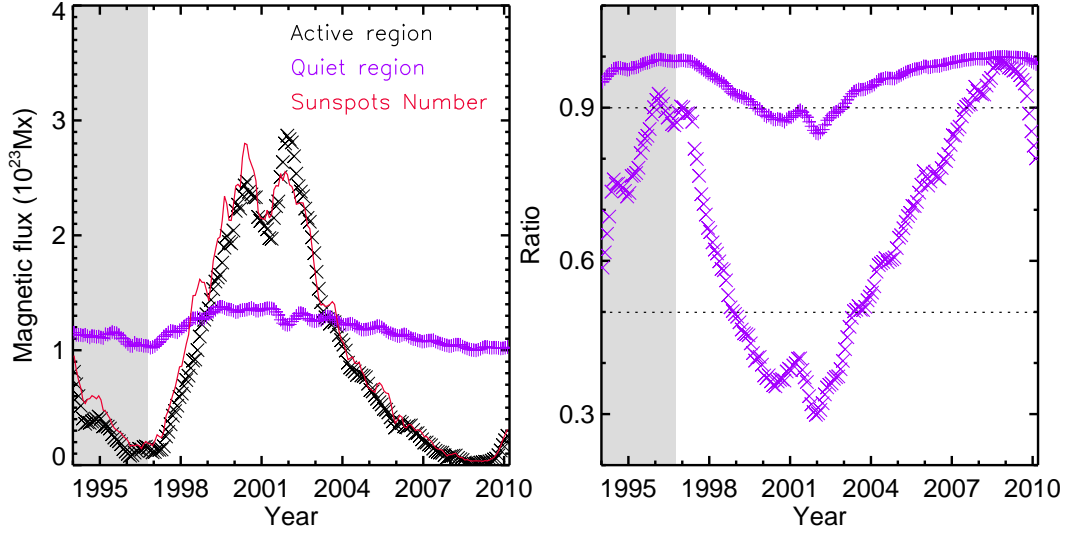


Fig. 2.— The left panel is the flux variations of ARs (cross symbols in black) and quiet Sun (‘+’ symbols in purple) in an interval including the entire 23rd Solar Cycle. The red curve represents the sunspot number changes in the cycle. The shaded columns are the statistical results based on the Kitt Peak full-disk magnetograms. The magnetic flux for quiet regions rises from 0.94×10^{23} Mx in December 1995 to 1.44×10^{23} in May 2002, increases by a factor of 1.53. The fractional quiet Sun area is shown by purple ‘+’ symbols, in the right panel. It decreases by a factor of 1.2 from the solar minima to maximum. The ratio of quiet Sun flux to the total Sun’s flux, the flux occupation of the quiet Sun, is shown by purple cross symbols in the right panel. The quiet Sun flux has dominated the Sun’s magnetic flux for 7.92 years in the 12.5 year Cycle 23.

Table 1: Cyclic variation of the NT elements with different flux range

Category	Flux (in Mx)	Number ratio	Flux (ratio)	Cor.
No-correlation	$(1.5\text{--}2.9)\times 10^{18}$	0.58%	6.48×10^{21} (0.05%)	-0.04
Anti-correlation	$(2.9\text{--}32.0)\times 10^{18}$	77.19%	4.72×10^{24} (37.40%)	-0.45
Transition	$(3.20\text{--}4.27)\times 10^{19}$	6.59%	1.15×10^{24} (9.08%)	-0.03
correlation	$(4.27\text{--}38.01)\times 10^{19}$	15.65%	6.74×10^{24} (53.46%)	0.82

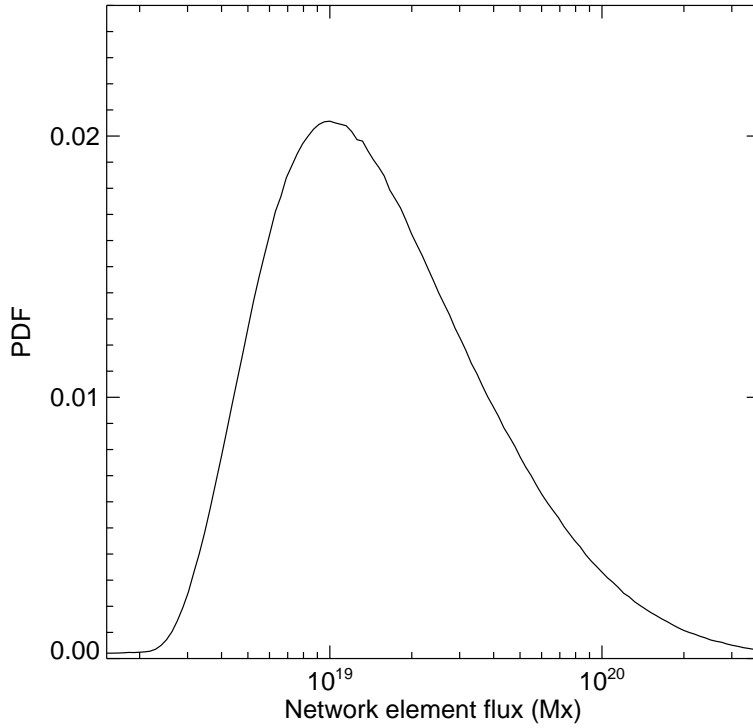


Fig. 3.— The probability distribution function of element magnetic flux for all the selected network elements during the interval from September 1996 to February 2010, i.e., average PDF of the quiet Sun’s small-scale magnetic elements. The peak distribution at 10^{19} Mx is consistent with that found for multiple MDI full-disk datasets by Parnell et al. (2009).

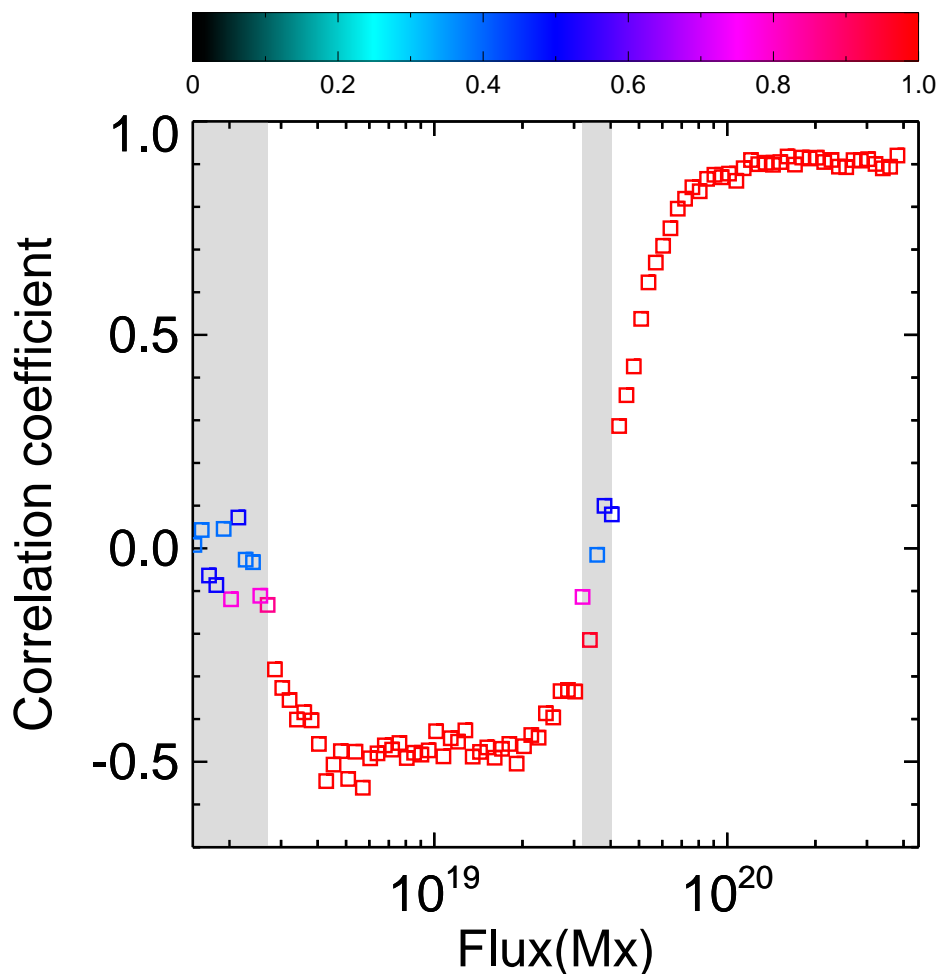


Fig. 4.— Correlation coefficients between the sunspot number and network element number of each of the 96 sub-group elements which are reconstructed according to the flux per element. There appears a 3-fold correlation scheme between the network elements and the sunspot cycle: basically no-correlation, anti-correlation and correlation. At the low end of flux spectrum, there are very small correlation coefficients. With the increasing flux per element, the correlation coefficients reach approximately to -0.58, then they become positive and reach as high as 0.92 after a very narrow transition in the flux range of $(3.20-4.27) \times 10^{19}$ Mx. The color bar represents the confidence level.

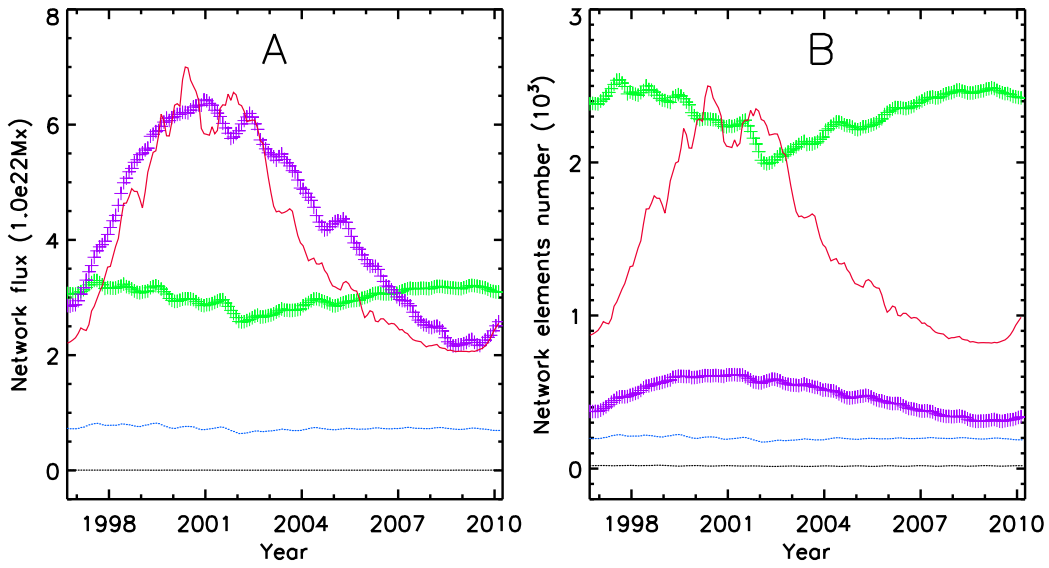


Fig. 5.— Cyclic variations of network element number (right panel) and flux (left panel) of 4 categories of network elements shown in Table 1, which represents the 3-fold correlation scheme of network elements with the sunspot cycle. The green ‘+’ is referring anti-correlation component elements, while the purple ‘+’ is for the in-phase correlation component elements. Black and blue dotted lines are elements which have no correlation or shown transition from anti-correlation to correlation with the solar cycle.

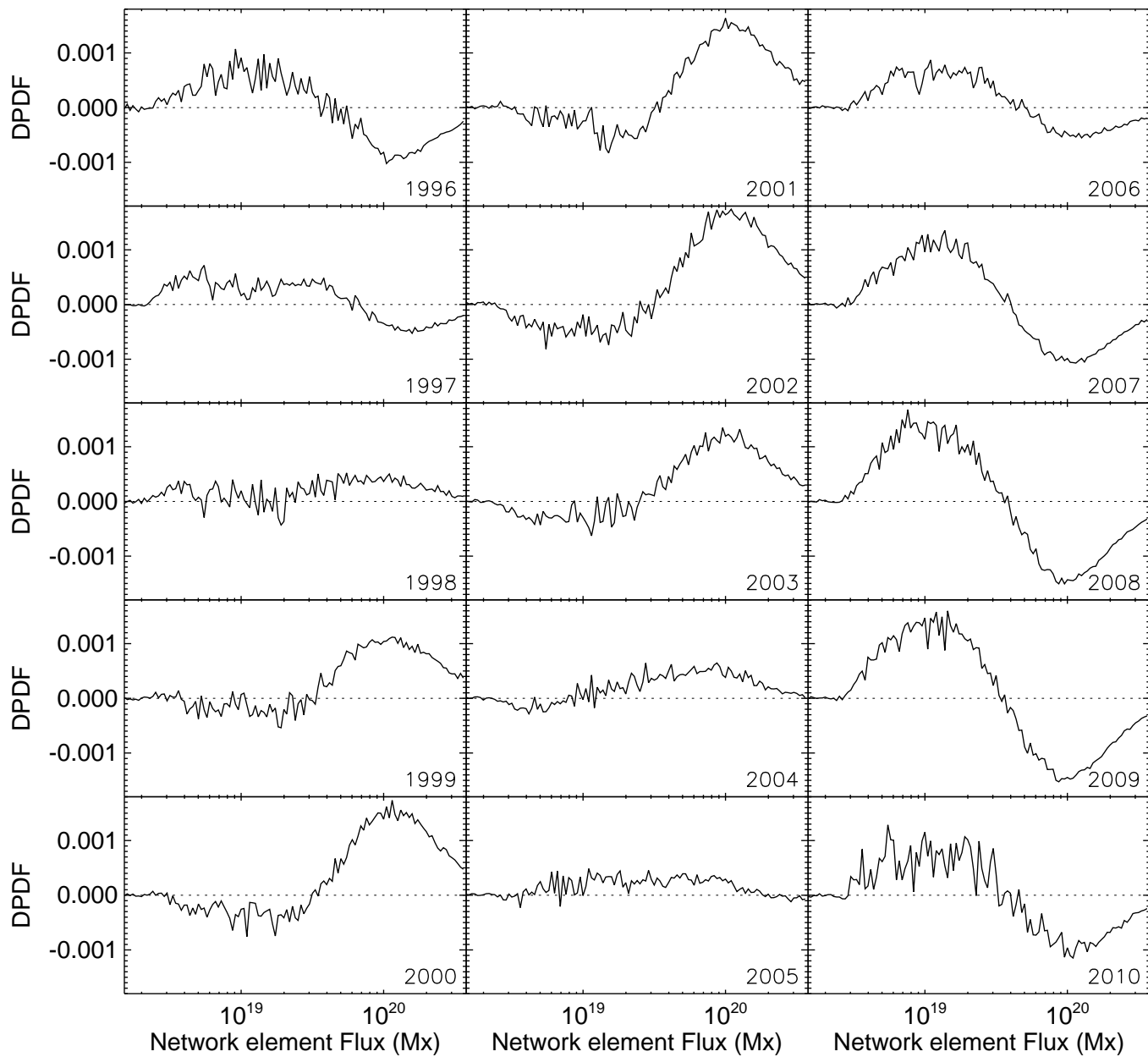


Fig. 6.— The differential probability distribution function (DPDF), i.e., the difference between the PDFs of yearly network magnetic elements and average PDF shown in Fig.3.